

Effect of synergistic CeO₂/MoS₂ abrasives on surface roughness and material removal rate of quartz glass



Gong Lv^a, Shengsheng Liu^a, Yuxi Cao^a, Zefang Zhang^{a,b}, Xufeng Li^{a,c}, Yufei Zhang^a, Tong Liu^{a,***}, Baosheng Liu^{a,***}, Kaiyue Wang^{a,*}

^a School of Materials Science and Engineering, Taiyuan University of Science and Technology, Taiyuan, 030024, Shanxi, China

^b Shanghai Yingzhi Polishing Materials Co.Ltd., Qingpu District, Shanghai, 201700, China

^c Shuozhou Industrial Technology Research Institute, Shuozhou, 036025, Shanxi, China

ARTICLE INFO

Handling Editor: P. Vincenzini

Keywords:

Quartz glass
CeO₂
MoS₂
Chemical mechanical polishing
Potassium oleate

ABSTRACT

Cerium oxide (CeO₂) is a primary abrasive frequently used in quartz glass polishing slurry for facilitating glass surface planarisation. However, due to its exorbitant synthesis costs and extremely corrosive as well as toxic reagents in the system, the chemical modification of CeO₂ abrasives have limited practical applications. In this work, a novel chemical mechanical polishing slurry for quartz glass incorporating potassium oleate (KOL), deionised water (DIW), cerium dioxide and molybdenum disulphide (MoS₂) was developed in this paper to enhance the chemical mechanical polishing (CMP) performance of CeO₂-based polishing slurry. KOL creates an alkaline environment for the system, further develops silicate insoluble substances on the quartz glass surface and boosts the material removal rate (MRR) in CMP. MoS₂ exhibits a two-dimensional layered nanosheet structure between the abrasive and quartz glass, and then acts as a solid lubricant to prevent excessive mechanical damage, thus increasing the abrasive's wettability. This characteristic helps avoid scratches and other defects on the quartz glass surface. Notably, when the content of KOL and MoS₂ in the system is 0.2 wt% and 0.3 wt%, respectively, the surface roughness of the quartz glass surface is 0.48 nm under the scanning area of 15 × 15 μm² and the MRR is 24.03 μm/h following CMP. The synergistic interaction between CeO₂ and MoS₂ significantly enhances the abrasive performance on the glass substrate, offering a novel approach for developing polishing fluids that leverage the collaborative effects between abrasives and two-dimensional materials.

1. Introduction

Quartz glass has recently gained prominence in precision engineering fields such as optoelectronics [1], semiconductor manufacturing [2] and high-end equipment [3,4]. As it has an increasingly broad range of applications in modern science and technology, the surface quality requirements of the quartz glass are getting stricter [5]. The traditional surface processing technology using indentation and wear mechanisms [6] is unsuitable for quartz glass, which exhibits hard and brittle properties [7]. It can easily result in defects such as pits or scratches on the glass surface, which inevitably affect the reliability and service life of precision equipment. Chemical mechanical polishing (CMP) technology combines chemical corrosion and mechanical friction. It eliminates defects on the material surface by using chemical reagents to initiate

chemical reactions on the material surface during mechanical polishing [8,9]. Therefore, using CMP technology can substantially enhance the quality of the material surface and obtain sub-micron or even nanometre surface roughness [10]. Due to its specific high flatness and precision controllability, CMP technology is an effective method to obtain a smooth quartz glass surface. The CMP slurry used in the polishing process plays a key role in the polishing performance; the slurry is a special mixture composed of abrasives and other chemical additives, which can effectively control the reaction process. Cerium oxide (CeO₂) [11], alumina [12] and silica [13] are widely used as abrasives in the polishing slurry. Because CeO₂ can react with the glass surface, it can be withdrawn rapidly under shear force; therefore, CeO₂ is the primary abrasive of quartz glass in the CMP process.

Many researchers use physical or chemical methods to modify the

* Corresponding author.

** Corresponding author.

*** Corresponding author.

E-mail addresses: 2023030@tyust.edu.cn (T. Liu), liubaosheng@tyust.edu.cn (B. Liu), wangkaiyue8@163.com (K. Wang).

abrasive surface to refine the material removal rate (MRR) and surface quality of CeO₂ slurry. Yuan et al. [14] created a series of composite abrasives termed zeolite imidazolium cerium oxide (CeO₂@ZIF-8) by depositing varying amounts of zeolitic imidazolate framework (ZIF-8) material on cerium oxide particles. This activity not only maintains the performance advantages of the original materials, but also strengthens their reactivity and dispersion. However, the surface roughness of quartz glass is only 1.23 nm. Xu et al. [15] synthesised uniform nanometre-sized CeO₂ abrasives using a hydrothermal method to increase the surface quality of polished quartz. Lanthanide elements and alkaline earth metals can manufacture solid solutions or composites with other polar or non-polar dielectrics [16,17]. In addition, researchers also doped them into CeO₂ for modification. The CeO₂ abrasive with a core-shell structure is also under the academic spotlight. Li et al. [18] proposed a new RE³⁺-doped core-shell CeO₂ abrasive system, to alter the ratio of Ce³⁺ and Ce⁴⁺ concentrations in CeO₂ abrasive to achieve a good MRR and surface quality. Unlike the defects of high leakage current, high tangential loss and structural distortion caused by oxygen vacancies in some multiferroic materials [19,20], the oxygen vacancies in CeO₂ abrasives will increase the concentration of Ce³⁺, thereby enhancing its reactivity with quartz glass. Although researchers use numerous inorganic and organic substances to transform the abrasive to boost its performance, it remains unfeasible to the environment due to high synthesis costs and low yield, and the system contains highly corrosive and toxic reagents [21]. Therefore, the large-scale production of modified CeO₂ abrasives is still challenging, which restricts the practical applications. Moreover, developing a quartz glass polishing slurry with simple components and environmental friendliness, which can rapidly upgrade the material removal efficiency and surface quality, has gradually captured researchers' attention.

Lubrication is the most effective method to control friction and wear, enhance the removal efficiency of quartz glass materials, and decrease the surface roughness and wear between the abrasive and workpiece [22,23]. Furthermore, two-dimensional materials with a layered structure [24], such as graphite [25] and molybdenum disulphide (MoS₂) [26,27], exhibit weak van der Waals forces between layers, allowing for relative sliding under shear force, displaying lubrication effects and bolstering their common application as solid lubricants [28]. In addition, compared with other materials, it makes them easier to adsorb to the substrate surface for effectively executing its lubricating effect [29]. MoS₂ exhibits excellent wear resistance, efficiently reducing friction surface wear with minimal volatilisation and loss [30]. In addition, it can sustain a stable lubrication performance under high pressure, speed and harsh conditions, thereby extending the lifespan of mechanical components [31,32]. This material holds significant promise for applications in lubrication and wear resistance. However, few studies have focused on the potential applications of MoS₂ in developing simple and effective polishing slurry, especially in quartz glass CMP. In addition, chemical additives that are not detrimental to people and the environment should also receive due attention. Potassium oleate [33] is derived from vegetable oil and exerts minimal impact on the environment and organisms. Moreover, it can provide an alkaline environment for quartz glass, generating a softened layer that is easier to remove during CMP. Therefore, in an alkaline environment created by potassium oleate, adding a MoS₂ two-dimensional material into CeO₂-based polishing slurry and using its wear resistance and lubricity to improve the MRR and surface quality of quartz glass in CMP processes requires research attention.

In this work, a CMP slurry for quartz glass polishing was developed by integrating MoS₂ nanomaterials with CeO₂ slurry and surfactant potassium oleate and DIW. To understand the effect of MoS₂ on polishing performance, we decided to add different contents of MoS₂ in CeO₂-based slurry to obtain the novel polishing slurry. A fixed content of potassium oleate can create the same alkaline environment in the polishing slurry with different contents of MoS₂. The glass surface morphology and material removal efficiency after using the new

polishing slurry and the traditional polishing slurry were compared. In comparison to the conventional CeO₂ slurry, the new slurry has a higher MRR and higher surface quality. Scanning electron microscopy (SEM) and transmission electron microscopy (TEM) were applied to characterise CeO₂/MoS₂ abrasives. The surface morphology and roughness of polished quartz glass were examined using an atomic force microscope (AFM). X-ray photoelectron spectroscopy (XPS), Fourier transform infrared spectroscopy (FTIR) and contact angle measurement further discussed the mechanism of improving the polishing performance.

2. Experimental details

2.1. Materials

Quartz glass (Xuzhong Quartz Products Co., Ltd., China) were processed into circular pieces with a diameter of 10 mm as the sample. Commercial calcined CeO₂ nanopowder with a mean size of ~80 nm was received from Zhongye New Materials Co., Ltd., China. MoS₂ nanopowder (purity ≥99.5 %), NaOH (purity 97 %) and potassium oleate (KOL, purity 98 %) power was purchased from Shanghai Macklin Biochemical Technology Co., Ltd., China. Polyurethane pads used in the experiments were supplied by Shenyang Kejing Auto-instrument Co., Ltd., China. Deionised water (DIW) was used throughout all the experiments, and all chemicals were used without any further purification.

2.2. Methods

In this work, the quartz glass was processed by five CMP slurries, and their polishing abilities were subsequently tested and examined. The CMP slurries were mechanically swirled continuously during the experiment to avoid the deposition of abrasives. These slurries contained an abrasive made from commercially available calcined CeO₂. In this experiment, five groups of the polishing slurry were designed: S1, S2, S3, S4 and S5. NaOH was used in slurry S1 as a pH regulator and 0.2 wt% KOL was added to the other slurries to create an alkaline polishing environment. The initial slurry was prepared by adding 4 wt% CeO₂ to deionised water, and adding 0 wt%, 0.1 wt%, 0.3 wt%, 0.5 wt% MoS₂ to S2, S3, S4 and S5 in turn. Then, it was stirred with a glass rod until the reagent dissolved and dispersed the powder. All these slurries have the same alkalinity of ~10. The mixture was then ultrasonically treated and mixed for 20 min for a uniform suspension. The performance and polishing effect of the S1–S5 polishing slurry were verified using the CMP polishing process diagram displayed in Fig. 1, as outlined in the experimental methodology. Fig. 1 (a) illustrates the S1–S5 CMP slurry preparation process. In CMP experiments, five small round blocks were evenly attached to the counterweight tray with paraffin for the best polishing effect (Fig. 1 (b)).

All experiments were performed using a precision lapping/polishing machine (UNIPOL-802, Shenyang Kejing Auto-instrument Co., Ltd., China). The slurry was conveyed by using a digital peristaltic pump/digital peristaltic pump (BT-300EA, Chongqing Jieheng Peristaltic Pump Co., Ltd., China). The sample was ultrasonically washed with DIW and absolute ethanol for 10 min to remove residues after process. The polyurethane pad was utilized in the CMP process, and the ideal process parameters, including the polishing disk rotation speed, polishing pressure, CMP slurry feed rate, and polishing time, were set as follows (see Table 1).

2.3. Characterization

The surface morphologies and sizes of CeO₂ and MoS₂ were observed by SEM (S4800, Hitachi, Japan) and TEM (JEM-F200, JEOL, Japan). The sessile drop method was used to determine the contact angles of the five CMP slurries on the surface of quartz glass, and a drop shape analyzer (DSA25R, KRUESS Scientific, Germany) was used to measure the drop shapes. Droplet shape and contact angle are analyzed by using

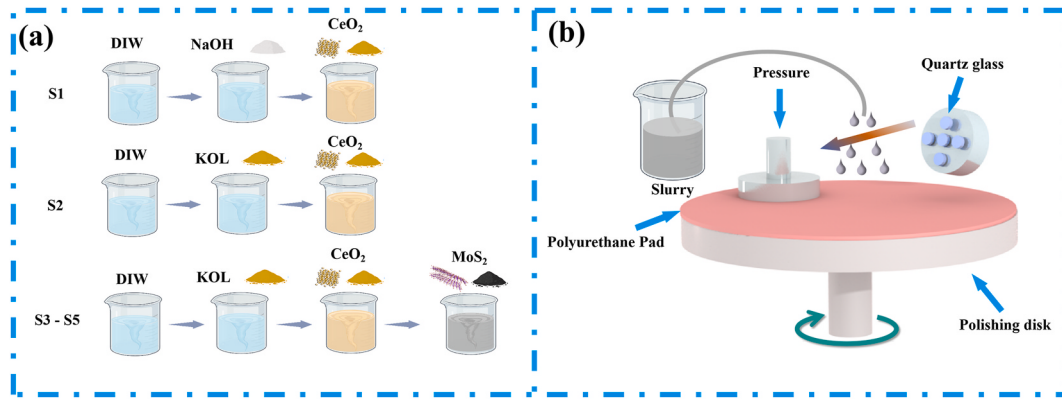


Fig. 1. Schematic illustration of CMP process for glass substrates. (a) Slurry preparation process, (b) CMP experimental setup.

Table 1

Process parameters of the polishing experiment.

Parameter	Value
Amount of slurry	300 g
Polishing disk rotation speed	90 rpm
Polishing pressure	1.35 kg
Polishing time	40 min
CMP slurry feed rate	15 mL/min

ADVANCE software. The measurement result is the average value of five repeated tests. Accordingly, the 3D surface profile and roughness were described and measured using an AFM (Dimension ICON, Bruker, Germany). The average value of surface roughness Ra at five randomly chosen sites was used as the measurement result to reduce measurement error.

Both the valence state of slurry before and after CMP and the elemental composition of quartz glass surface were analyzed by XPS (Axis Supra, Shimadzu, Japan). By using monochromatic Al K α radiation to obtain XPS spectra, all binding energies were calibrated by applying an external C1s signal of 284.8 eV before analysis. The FTIR spectrometer (INVENIO, Bruker, Germany) was used to analyze the vibration peaks of quartz glass, KOL, quartz glass treated with potassium oleate and quartz glass treated with slurry. The range of infrared absorption spectrum was 400–4000 cm $^{-1}$.

The MRR ($\mu\text{m}\cdot\text{h}^{-1}$) of the quartz glass sample, which is obtained from the mass loss of the sample before and after each CMP, can be determined from Eq. (1) [14]:

$$MRR = \frac{\Delta m}{\rho \cdot S \cdot t} \times 10^4 \quad (1)$$

Where MRR is the material removal rate, Δm (g) is the mass loss of quartz sample during CMP, ρ is the density of quartz sample with a value of 2.2 g·cm $^{-3}$, S (cm $^{-2}$) is polishing contact area, and t (h) is polishing time.

3. Results and discussion

3.1. Structure and morphology analysis of CeO₂ and MoS₂

The CeO₂ abrasive and MoS₂ in the CMP polishing slurry were characterised using SEM and TEM. The shape and size of CeO₂ nanoparticles can be observed in Fig. 2(a) and (b). The polishing characteristics of CeO₂-based abrasives largely depend on its size and shape [15], which also impact the polishing effect and surface quality. Abrasives with larger particle sizes are commonly used to eliminate substantial surface imperfections, swiftly diminishing the surface roughness. Nonetheless, coarse abrasives may result in deep scratches or uneven surfaces. Abrasives with smaller particle sizes can effectively eliminate minute surface defects. Abrasives with smaller particle sizes can yield a more uniform polishing effect; however, they are less efficient in material removal, often necessitating extended polishing periods [34]. Regulating the size morphology of conventional ceria abrasives via calcination has proven challenging. Therefore, the SEM image in Fig. 2(a) shows that the CeO₂ abrasive shape is close to the spherical shape; its

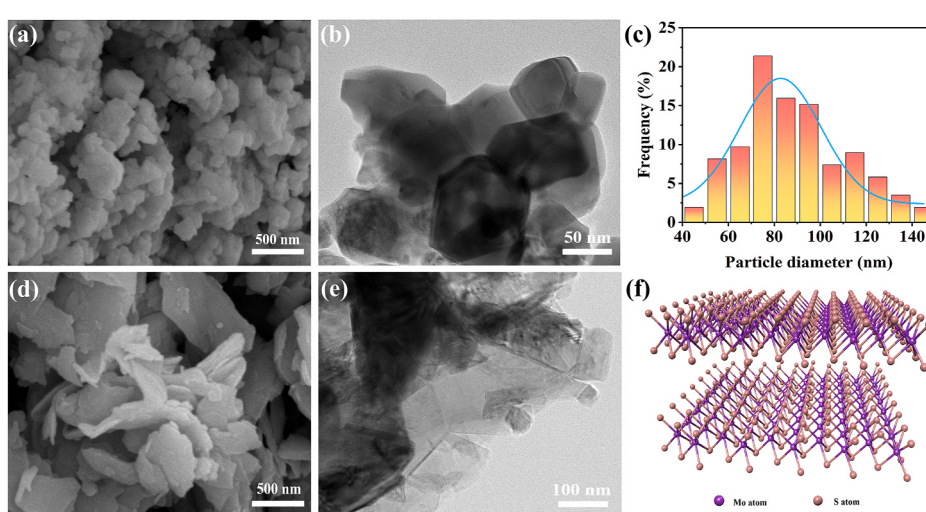


Fig. 2. (a) SEM, (b) TEM images, and (c) diameter distribution of CeO₂, and (d) SEM, (e) TEM images of MoS₂, (f) molecular structure of MoS₂.

shape is uneven. The TEM image in Fig. 2 (b) more clearly described the CeO₂ abrasive edge as having prominent edges and corners. Its irregular shape and sharp edges usually make the cutting more effective in polishing, and may cause scratches or other mechanical damage in the material removal process [35]. Due to their irregular shape and sharp edges, these abrasives often cut more effectively during polishing. They may lead to scratches or other mechanical damage during the material removal [36]. Ce⁴⁺ can be reduced to Ce³⁺ in the system [37], leading to further physical and chemical reactions with the surface of quartz glass surface. The analysis of the CeO₂ particle size distribution histogram in Fig. 2 (c) reveals an average particle size of 83.62 nm. In addition, Fig. 2 (d) and (e) illustrate that MoS₂ is a nanomaterial with a lamellar structure. MoS₂ has a high specific surface area, which makes it cover a larger surface area than other nanomaterials while carrying CeO₂ abrasive. The two adjacent layers of the MoS₂ structure are combined by weak van der Waals force, making it simpler for the adjacent layers to slide each other under shear force to generate a lubrication effect. The atoms in the same atomic layer are covalently bonded, and each layer comprises of molybdenum atoms surrounded by six sulphur atoms, creating an octahedral structure (Fig. 2 (f)), which contributes to its excellent lubricity and mechanical properties [30].

EDS mapping was used to characterise and effectively depict the distribution of CeO₂/MoS₂ abrasives. Fig. 3 displays the EDS mapping images. The TEM images showed irregularly shaped nanoparticles on the surface layer, and the corresponding elements were Ce and O. EDS also revealed Mo and S elements at the bottom of the nanoparticles, demonstrating that the CeO₂ abrasives are transported by MoS₂ nanosheets. In the chemical mechanical polishing (CMP) process of quartz glass, MoS₂ as a solid lubricant increases the abrasive's fluidity and prevents excessive damage on the surface of quartz glass surface.

3.2. Characterization of slurry

The polishing slurry of S1–S5 was prepared according to the experiment, and the contact angle of S1–S5 was measured with quartz glass as the substrate. Fig. 4 shows that the average contact angle of polishing solution S1 was 49.7°. After adding MoS₂ two-dimensional material and KOL, the slurry of S2–S5 demonstrated a lower contact angle than S1. The findings are consistent with those reported in the literature [38]. Excellent wettability can enhance the wetting performance between the polishing slurry and quartz glass in the polishing process and then facilitate the propagation and diffusion of slurry on the solid surface [39]. The most likely reason for this outcome is that KOL exists in the system as a surfactant, and its molecular structure comprises a long-chain fatty acid radical ion and potassium ion. The fatty acid radical ion is a long-chain alkyl structure comprising 17 carbon atoms with an unsaturated bond. Its unique structure makes it hydrophilic to a certain extent, reducing the polishing solution's surface tension and creating a stable suspension [40].

3.3. Analysis of CMP performance

MRR and Ra are crucial indicators used to evaluate the polishing performance. Fig. 5 shows the investigation of the MRR effect of slurry S1–S5 on quartz glass. The MRR after adding MoS₂ nanosheets in the

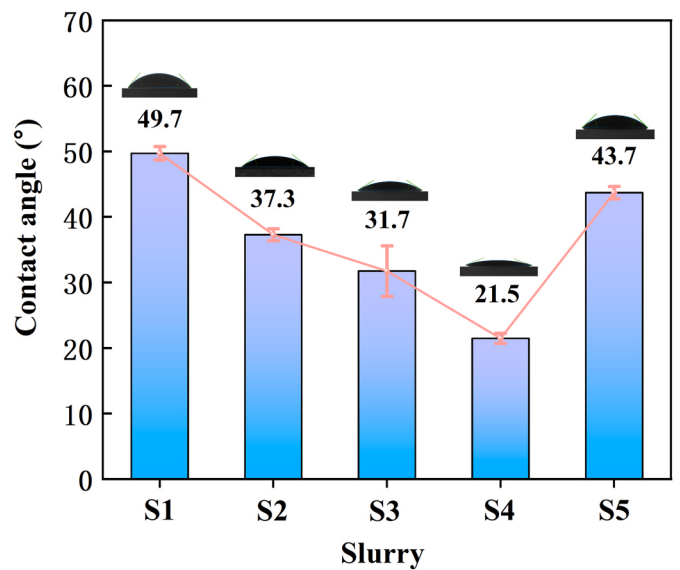


Fig. 4. Contact angle of polishing slurry S1–S5 for glass substrate.

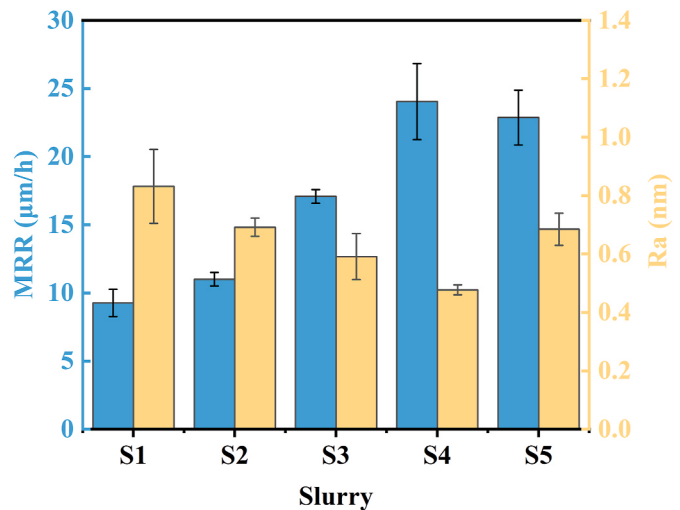


Fig. 5. The MRR and Ra of S1–S5 after CMP process.

polishing slurry was significantly higher than that of slurry without MoS₂. It share a qualitative relationship with the wettability of the polishing slurry shown in Fig. 4. The reduction of the contact angle can enhance the MRR of the polishing slurry to a certain extent, primarily because it can make more slurry contact with the surface of quartz glass while improving the wettability. The polishing effect obtained using the conventional CeO₂-based polishing slurry (S1) is not ideal. The MRR is only 9.27 μm/h and the surface roughness of 0.83 nm is obtained. Compared with S1, KOL in the slurry of S2–S5 can form more passivation layers with the quartz glass surface, which can be quickly removed

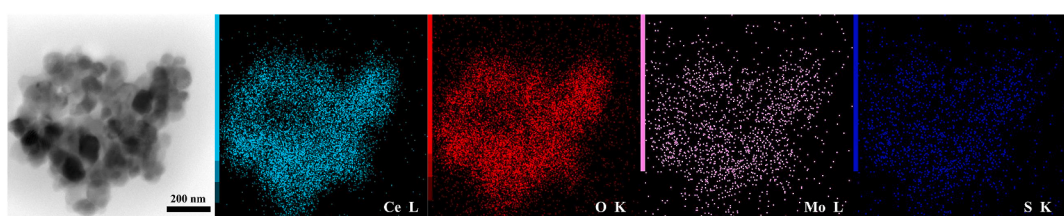


Fig. 3. Energy disperse spectroscopy (EDS) mapping images of the CeO₂/MoS₂ abrasives.

under the action of CeO_2 abrasive to boost the MRR of the polishing slurry. The polishing performance of S2 slurry has been significantly enhanced, with an MRR of $11 \mu\text{m}/\text{h}$ and surface quality of 0.69 nm . Fig. 5 displays that the MRR can reach $24.03 \mu\text{m}/\text{h}$ after adding 0.3 wt\% MoS_2 nanosheets, and the results are nearly twice as high as those reported in the literature [34]. Meanwhile, the surface quality was upgraded by adding MoS_2 nanosheets. S4 has the lowest Ra value of 0.48 nm with a measurement area $15 \times 15 \mu\text{m}^2$. Among the five kinds of slurry, slurry S4 generally exhibits the best polishing effect, with the lowest Ra and the largest MRR. Therefore, the best composition of the polishing slurry for quartz glass is 4.0 wt\% CeO_2 , 0.3 wt\% MoS_2 , 0.2 wt\% KOL and DIW. With the increasing content of MoS_2 nanosheets, Ra increased, whereas MRR of S5 ($22.87 \mu\text{m}/\text{h}$) was comparable with S4 slurry. The main possible explanation is that CeO_2 abrasive has an irregular shape, and its hardness is close to that of quartz glass, which is prone to mechanical damage during CMP. As a two-dimensional material, MoS_2 can act as a solid lubricant in the system to reduce the abrasive damage to quartz glass, including scratches and pits, and refine the surface quality. Under the experimental polishing pressure of 1.35 kg , the friction between the abrasive and quartz glass will be further reduced with the increase in the MoS_2 content in the system due to the hardness of MoS_2 being smaller than those of CeO_2 and quartz glass. This effect makes the motion mode of the CeO_2 abrasive change from sliding to rolling [21], and the MRR will remain unchanged after reaching the maximum value; therefore, the bulges and scratches on the glass surface cannot be removed. Hence, with the increase in the MoS_2 content, Ra will display a trend of first decreasing and then increasing.

Fig. 6(a-f) illustrates the three-dimensional surface profile of quartz glass before and after polishing with S1 suspension (pure CeO_2 polishing slurry) and S2-S5 suspension (MoS_2 and KOL polishing slurry). AFM revealed that there were scratches, bulges and other defects on the surface of quartz glass before CMP, the surface roughness was 2.65 nm with a measurement area of $15 \times 15 \mu\text{m}^2$. Compared with the quartz glass surface with significant roughness before polishing, the polishing effect of the polishing slurry (S2-S5) after adding MoS_2 and KOL is smoother without evident bulge. The surface quality of quartz glass was enhanced after CMP with S1 polishing slurry. The scratches and bulges on the quartz surface were substantially reduced. However, adding KOL as a surfactant further lowers the surface roughness, and S2 polishing slurry provides an excellent polishing effect. Moreover, after MoS_2 was introduced into the polishing slurry, the surface roughness of quartz glass decreased further. While using S4 polishing slurry (MoS_2 0.3 wt\%), the lowest Ra (Ra = 0.48 nm) can be obtained at the same time, meaning that S4 polishing slurry (MoS_2 0.3 wt\%) can effectively increase the

surface quality of polished glass. The 3D profile of AFM revealed almost negligible bumps and scratches on the surface. S4 obtained a smoother surface compared with other polishing slurries. MoS_2 can boost the lubrication performance in friction and wear, mitigating the hard damage of CeO_2 agglomeration to the glass substrate [41]. However, excessive MoS_2 will reduce the mechanical stress of the abrasive in the polishing solution on the quartz glass, further hindering the effective grinding of the glass surface roughness peak. Therefore, the S5-polished surface exhibited defects such as bulges that cannot be removed, thus increasing the surface roughness Ra value of quartz glass (Fig. 6 (f)). In other words, the addition of MoS_2 (a two-dimensional material) improves the polishing fluid system, which can achieve excellent polishing performance compared to some different methods of chemically modified abrasives [10,14].

3.4. Analysis of the polishing mechanism of quartz glass

Fig. 7 illustrates the XPS characteristic spectra of the new polishing slurry after adding MoS_2 . The valence states of Mo, S and O in the polishing slurry before and after polishing were measured using XPS. In Fig. 7 (a), the peaks of O 1s spectra of the polishing slurry at 531.04 eV and 528.97 eV corresponding to the O^{2-} of Ce^{3+} and Ce^{4+} in the system, respectively [15]. The Ce element has unfilled 4f orbitals; therefore, a part of Ce^{4+} in the aqueous solution will be converted to Ce^{3+} [37,42]. Under mechanical stress, the Ce^{3+} will react with the surface of quartz glass to achieve an ideal polishing effect. In the polished system, a new peak of O 1s at the binding energy of 532.1 eV is presented in Fig. 7 (b), the Ce-O-Si bond formed in the polishing process [43]. The primary reason is that Ce^{3+} in the polishing slurry can provide electrons to the anti-bond orbit of the Si-O bond on the surface of quartz glass during the polishing process, further weakening and stretching the Si-O bond. The Si-O bond is easier to break, forming more $\equiv \text{Si}-\text{OH}$ groups on the glass surface and promoting the formation of Ce-O-Si under the action of Ce^{3+} [14,44]. In addition, Fig. 7 (c) and (e) reveal that the XPS spectra of the S element and Mo element before polishing have the binding energies of 162.9 eV and 161.74 eV , respectively, in Fig. 7 (c) for the species S $2p_{1/2}$ and S $2p_{3/2}$, respectively. The Mo $3d_{3/2}$ and Mo $3d_{5/2}$ have binding energies (Fig. 7 (e)) of 232.04 eV and 228.89 eV , respectively. Fig. 7 (d) and (f) shows the XPS spectra of the S element and Mo elements after polishing. The binding energies of S $2p_{1/2}$ and S $2p_{3/2}$ are 162.64 eV and 161.48 eV , respectively. The binding energies of Mo $3d_{3/2}$ and Mo $3d_{5/2}$ are 231.78 eV and 228.63 eV , respectively. The corresponding peaks (Fig. 7 (d) and (f)) in the spectra of Mo 3d and S 2p in the slurry after cyclic polishing do not change, and have almost the

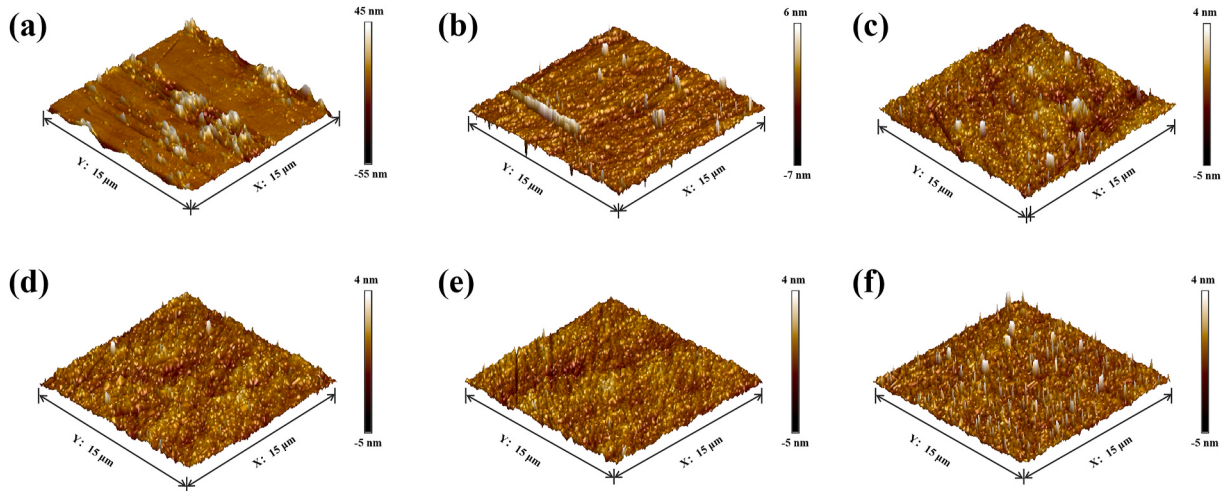


Fig. 6. Surface profile of glass substrates (a) before polished, Ra = 2.65 nm ; (b) polished by S1, Ra = 0.83 nm ; (c) polished by S2, Ra = 0.69 nm ; (d) polished by S3, Ra = 0.59 nm ; (e) polished by S4, Ra = 0.48 nm ; (f) polished by S5, Ra = 0.68 nm .

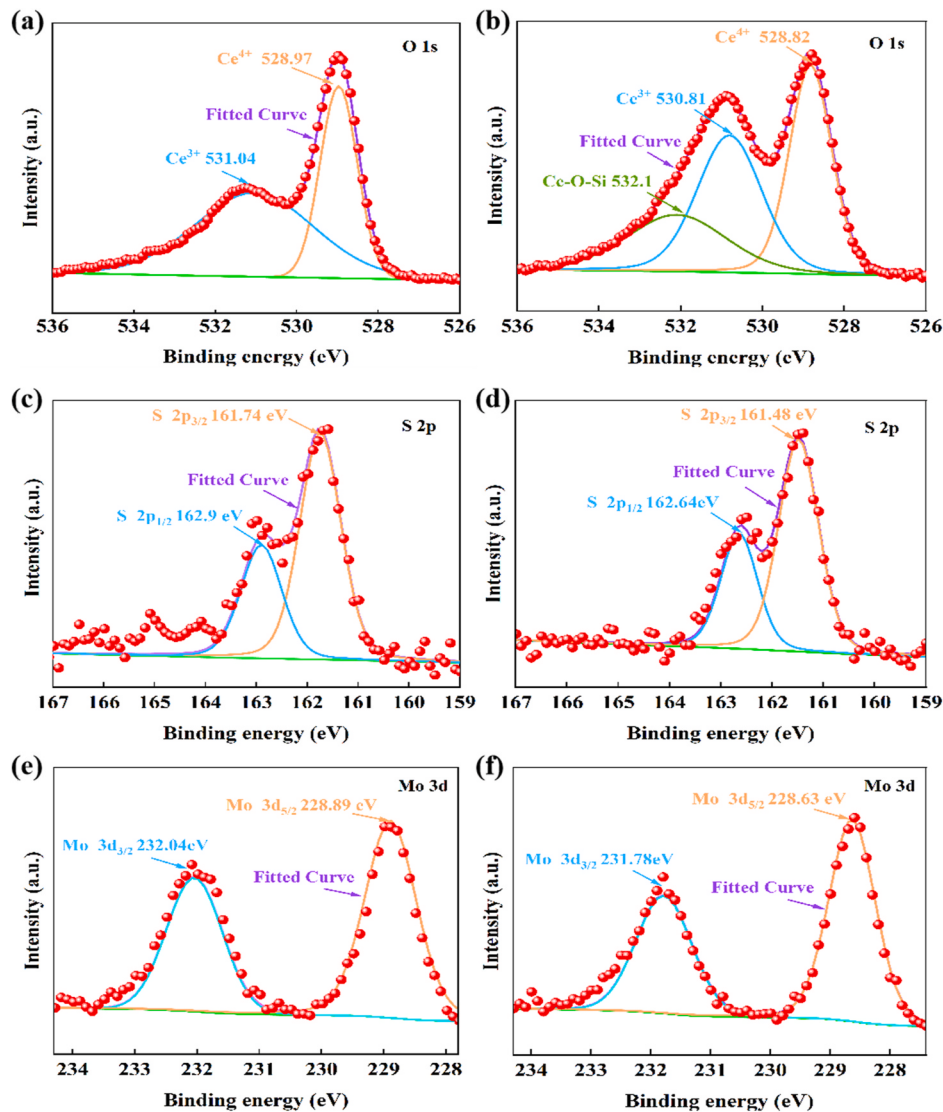
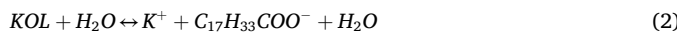


Fig. 7. XPS O 1s, S 2p and Mo 3d spectra of slurry (a,c,e) before and (b,d,f) after CMP.

same peaks. Therefore, it can be concluded that MoS₂ did not participate in any chemical reaction during the whole CMP process and only contributed towards the physical effect of lubrication.

Potassium oleate is used as a surfactant in polishing slurry. When oleic acid integrates with potassium ion to create potassium oleate, the hydrogen ion in the carboxyl group is replaced by a potassium ion to form a carboxylate, which makes potassium oleate alkaline. Therefore, potassium oleate in water exhibits alkaline properties [40]. It will undergo a hydrolysis reaction in the aqueous solution to produce potassium cation (K⁺) and oleate anion (C₁₇H₃₃COO⁻). Notably, oleate anion (C₁₇H₃₃COO⁻) can accept protons in the water system to create carboxylic acid compounds (C₁₇H₃₃COOH) and hydroxyl ions (OH⁻) to make the system alkaline and increase the system's pH value. The alkaline substances in the system can further react with quartz glass to develop silicate insoluble substances on the surface. The following equation can describe the relevant reaction mechanism [15,22]:



To determine whether a new species (SiO₃²⁻) is generated after the

surface of quartz glass is in contact with KOL solution, the elemental valence changes of quartz glass before and after immersion in KOL solution were examined by XPS spectra, to further evaluate the role of KOL and quartz glass in the CMP process. Fig. 8 (a) and (b) display the XPS spectra of Si and O elements of quartz glass before CMP. The main peak at 103.47 eV in Fig. 8 (a) is ascribed to Si 2p in SiO₂ [44]. Fig. 8 (b) shows two primary peaks at 533.08 eV and 532.48 eV, both attributed to O²⁻ [22,45]. SiO₂ is the only substance on the quartz glass surface. Fig. 8 (c) and (d) depict the XPS spectra of Si and O of quartz glass immersion in the KOL solution. Fig. 8 (c) illustrates two main peaks at 103.3 eV and 102.6 eV, of which 103.3 eV is identified as the relatively weak peak at Si 2p_{3/2}. The binding energy of 102.6 eV is considered as Si 2p_{3/2} in SiO₃²⁻ [14,15,18]. In Fig. 8 (d), the binding energy of 531.69 eV is deemed to be caused by SiO₃²⁻ [46]. The peaks at 533.6 eV and 531.07 eV result from the binding energy arising from O-C and O=C in potassium oxalate, respectively. The binding energy at 532.27 eV is identified as an O 1s signal from SiO₂, indicating that following the addition of the KOL solution, it can react with the surface of quartz glass to form new compounds.

The FTIR spectra shown in Fig. 9 were used to analyze the chemical interactions between the surface of quartz glass and CMP slurry. Fig. 9 (a) shows in detail the FTIR spectra of KOL samples used in this work. The band at 2847.3 cm⁻¹ corresponds to the symmetric stretching

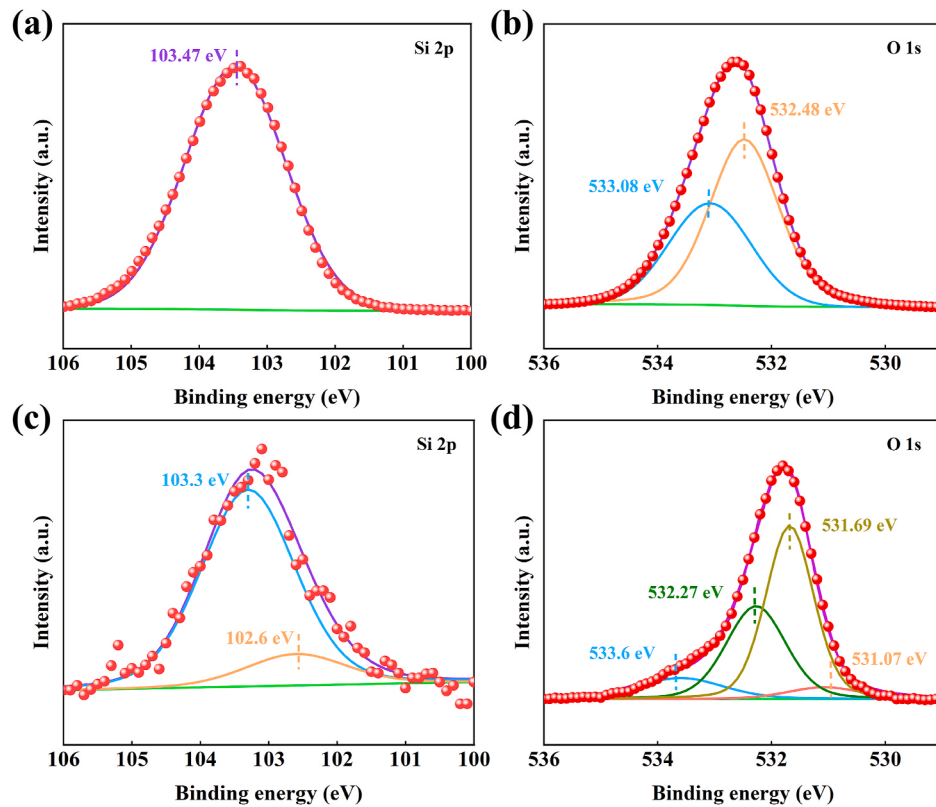


Fig. 8. XPS O 1s, Si 2p spectra of Si (a, c) before and (b, d) after immersion in KOL solution.

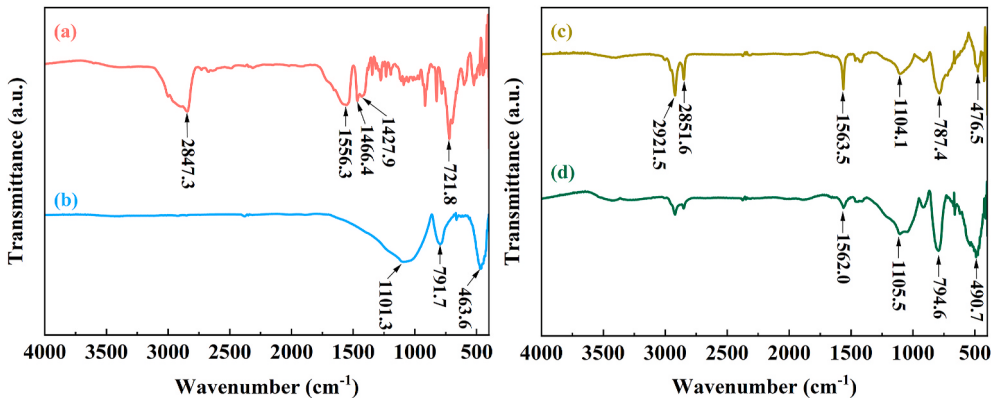


Fig. 9. FTIR spectra of (a) KOL, (b) Quartz glass sample, (c) Quartz glass treated with KOL, and (d) Quartz glass treated with slurry.

vibration of the C–H bond. The bands at 1556.3 cm⁻¹ and 1427.9 cm⁻¹ are related to the carboxyl absorption band, corresponding to the asymmetric and symmetric stretching vibrations of the –COO– group, respectively [47]. In addition, the two spectral bands at 1466.4 cm⁻¹ and 721.8 cm⁻¹ in Fig. 9 (b) belong to the shear vibration of the –CH₂– group and the rocking vibration of -(CH₂)_n ($n \geq 4$), respectively [22, 48]. In Fig. 9 (b), three significant peaks are concentrated at 1101.3 cm⁻¹, 791.7 cm⁻¹ and 463.6 cm⁻¹, which belong to the asymmetric tension, symmetric tension and bending models of Si–O–Si, respectively [49]. Fig. 9 (c) shows the FTIR spectra of quartz glass after immersion in KOL solution. The bands 1104.1 cm⁻¹, 787.4 cm⁻¹ and 476.5 cm⁻¹ are shifted from 1101.3 cm⁻¹, 791.7 cm⁻¹ and 463.6 cm⁻¹, respectively, of the original quartz glass sample in Fig. 9 (b), which is considered to be the interaction between quartz glass and KOL solution. The spectral bands at 1105.5 cm⁻¹, 794.6 cm⁻¹ and 490.7 cm⁻¹ after the reaction of quartz glass and CMP slurry in Fig. 9 (d) are also shifted compared with

Fig. 9 (c), primarily because Ce³⁺ generated after the addition of abrasive CeO₂ reacts with the quartz glass surface to create Ce–O–Si bond [48,50], which is consistent with the XPS spectra results in Fig. 7.

The conventional CeO₂-based polishing slurry can obtain a relatively flat surface by sliding cutting of the abrasive on the glass surface in the CMP process. In this case, the surface of quartz glass will produce some defects, such as scratches or micro-cracks, which are unfavourable for further production and application. In Fig. 10, due to the addition of KOL, the contact angle of the system is smaller, which increases the contact area with the glass substrate to achieve better mechanical effects and chemical reactions. Further more, it creates an alkaline environment for the system and enables the formation of more ≡ Si–OH groups on the surface. During the polishing process, Ce³⁺ provides electrons to the anti-bond orbit of the Si–O bond on the quartz glass surface, thus creating the Ce–O–Si bond under the action of Ce³⁺. The Ce–O–Si bond is stronger than Si–O–Si; therefore, the polishing process is completed

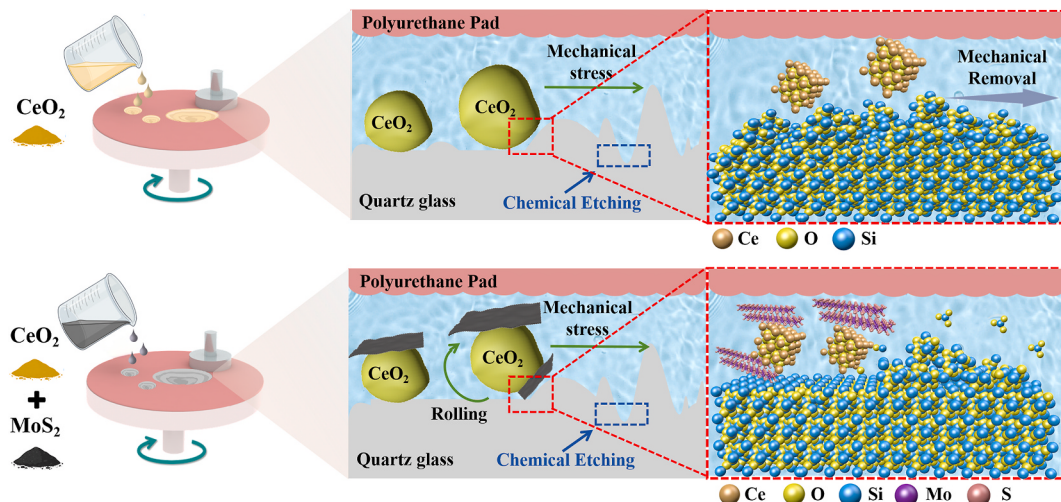


Fig. 10. Schematic diagram of CMP mechanism for quartz glass with slurry.

under mechanical stress [51]. Due to its unique structure, MoS_2 exists as a solid lubricant in the system during the polishing process. It acts between the abrasive, polishing pad and quartz glass to prevent excessive mechanical damage caused by the abrasive on the quartz glass surface, resulting in scratches and other defects. Simultaneously, it can also increase the fluidity and wettability of the abrasive. Thus, higher MRR and lower Ra than conventional CeO_2 -based slurry can be obtained. Therefore, the chemical and mechanical effects of the new polishing slurry are enhanced at the same time, which has excellent polishing performance.

4. Conclusions

In conclusion, a novel polishing slurry was developed by incorporating MoS_2 , CeO_2 , KOL and DIW. The effects of polishing slurry containing different MoS_2 concentrations on the polishing performance of quartz glass were studied in this paper. According to the SEM and TEM images, CeO_2 abrasive was carried by MoS_2 nanosheets. The contact angle test shows that the best wettability can be obtained when the MoS_2 content is 0.3 wt% on the glass substrate. The polishing experiment revealed that the slurry containing MoS_2 exhibits excellent polishing performance. When the content of MoS_2 in the slurry increased to 0.3 wt %, Ra significantly decreased to the low value of 0.48 nm, and the high MRR of 24.03 $\mu\text{m}/\text{h}$ was achieved. Finally, the removal mechanism was investigated using XPS and FTIR analysis. Adding KOL enhanced the wettability between the polishing solution and the glass substrate and provided OH^- ions for the system. The alkaline substances in the system develop silicate insoluble substances on the quartz glass surface. MoS_2 only acts as a solid lubricant to enhance the lubricity between the abrasive, polishing pad and quartz glass surface. It does not participate in any chemical reaction. Therefore, the scratch and micro-cracks of CeO_2 abrasive under mechanical stress are reduced. The synergistic effect between the components gives quartz glass polishing an excellent CMP performance. This work introduces MoS_2 as a solid lubricant in the CMP process for the first time, which proposes a novel idea for developing a polishing slurry to minimise polishing scratches and enhance the surface quality of quartz glass.

CRediT authorship contribution statement

Gong Lv: Visualization, Investigation, Formal analysis, Data curation. **Shengsheng Liu:** Formal analysis, Data curation, Conceptualization. **Yuxi Cao:** Supervision, Methodology, Conceptualization. **Zefang Zhang:** Visualization, Supervision, Methodology. **Xufeng Li:** Visualization, Methodology, Investigation. **Yufei Zhang:** Investigation, Data curation. **Tong Liu:** Supervision, Methodology, Conceptualization.

Baosheng Liu: Visualization, Supervision, Funding acquisition. **Kaiyue Wang:** Visualization, Supervision, Project administration, Methodology, Funding acquisition.

Declaration of competing interest

The authors declare that they have no known competing financial interests or personal relationships that could have appeared to influence the work reported in this paper.

Acknowledgments

This work was supported by the Major Science and Technology Project of Shanxi Province (No. 202301030201001).

References

- [1] Y. Zheng, P. Ma, H.B. Li, Z.C. Liu, S.L. Chen, Studies on transmitted beam modulation effect from laser induced damage on fused silica optics, Opt Express 21 (2013) 16605–16614, <https://doi.org/10.1364/oe.21.016605>.
- [2] R. Kitamura, L. Pilon, M. Jonasz, Optical constants of silica glass from extreme ultraviolet to far infrared at near room temperature, Appl. Opt. 46 (2007) 8118–8133, <https://doi.org/10.1364/ao.46.008118>.
- [3] F. Kotz, N. Schneider, A. Striegel, A. Wolfschläger, N. Keller, M. Worgull, W. Bauer, D. Schild, M. Milich, C. Greiner, D. Helmrich, B.E. Rapp, Glassomer-processing fused silica glass like a polymer, Adv. Mater. 30 (2018) 1707100, <https://doi.org/10.1002/adma.201707100>.
- [4] S. Joshi, A. Shukla, N. Kumar, R. Choudhary, Nd substitution response on structural, dielectric, and electrical features of bismuth iron titanate, Ceram. Int. 50 (2024) 1643–1654, <https://doi.org/10.1016/j.ceramint.2023.10.259>.
- [5] X. Feng, D.C. Sayle, Z.L. Wang, M.S. Paras, B. Santora, A.C. Sutorik, T.X.T. Sayle, Y. Yang, Y. Ding, X. Wang, Y.-S. Her, Converting ceria polyhedral nanoparticles into single-crystal nanospheres, Science (New York, N.Y.) 312 (2006) 1504–1508, <https://doi.org/10.1126/science.1125767>.
- [6] S.K. Patel, B. Kuriachen, N. Kumar, R. Nateriya, The slurry abrasive wear behaviour and microstructural analysis of A2024-SiC-ZrSiO₄ metal matrix composite, Ceram. Int. 44 (2018) 6426–6432, <https://doi.org/10.1016/j.ceramint.2018.01.037>.
- [7] N. Kumar, A. Shukla, R. Choudhary, Structural, dielectric, electrical and magnetic characteristics of lead-free multiferroic: Bi(Cd_{0.5}Ti_{0.5})O₃-BiFeO₃ solid solution, J. Alloys Compd. 747 (2018) 895–904, <https://doi.org/10.1016/j.jallcom.2018.03.114>.
- [8] Z.Y. Zhang, J.F. Cui, J.B. Zhang, D.D. Liu, Z.J. Yu, D.M. Guo, Environment friendly chemical mechanical polishing of copper, Appl. Surf. Sci. 467 (2019) 5–11, <https://doi.org/10.1016/j.apsusc.2018.10.133>.
- [9] P. Zhang, G.M. Chen, Z.F. Ni, Y.G. Wang, K. Teng, S.H. Qian, D. Bian, Y. Zhao, The effect of Cu²⁺ ions and Glycine complex on chemical mechanical polishing (CMP) performance of SiC substrates, Tribol. Lett. 69 (2021) 94, <https://doi.org/10.1007/s11249-021-01468-0>.
- [10] X.Y. Yuan, H. Lei, C.D. Chen, An ethylenediaminetetraacetic acid (EDTA) surface-functionalized CeO_2 composite abrasives with the effective improvement of the removal rate on glass CMP, Ceram. Int. 50 (2024) 293–305, <https://doi.org/10.1016/j.ceramint.2023.10.103>.

- [11] P. Janos, J. Ederer, V. Pilarová, J. Henych, J. Tolasz, D. Milde, T. Opletal, Chemical mechanical glass polishing with cerium oxide: effect of selected physico-chemical characteristics on polishing efficiency, *Wear* 362 (2016) 114–120, <https://doi.org/10.1016/j.wear.2016.05.020>.
- [12] N. Brahma, J.B. Talbot, Effects of CMP slurry additives on the agglomeration of alumina nanoparticles 1: general aggregation rate behavior, *J. Colloid Interface Sci.* 419 (2014) 56–60, <https://doi.org/10.1016/j.jcis.2013.12.029>.
- [13] L. Xu, H. Lei, Nano-scale surface of ZrO_2 ceramics achieved efficiently by peanut-shaped and heart-shaped SiO_2 abrasives through chemical mechanical polishing, *Ceram. Int.* 46 (2020) 13297–13306, <https://doi.org/10.1016/j.ceramint.2020.02.108>.
- [14] X.Y. Yuan, C.D. Chen, H. Lei, Z.F. Zhang, Synthesis, characterization of $CeO_2@ZIF-8$ composite abrasives and their chemical mechanical polishing behavior on glass substrate, *Ceram. Int.* 49 (2023) 5189–5198, <https://doi.org/10.1016/j.ceramint.2022.10.037>.
- [15] G.H. Xu, Z.Y. Zhang, F.N. Meng, L. Liu, D.D. Liu, C.J. Shi, X.X. Cui, J.M. Wang, W. Wen, Atomic-scale surface of fused silica induced by chemical mechanical polishing with controlled size spherical ceria abrasives, *J. Manuf. Process.* 85 (2023) 783–792, <https://doi.org/10.1016/j.jmapro.2022.12.008>.
- [16] N. Kumar, A. Shukla, R. Choudhary, Structural, dielectric, electrical and magnetic characteristics of lead-free multiferroic: $Bi(Cd_{0.5}Ti_{0.5})_3\cdot BiFeO_3$ solid solution, *J. Alloys Compd.* 747 (2018) 895–904, <https://doi.org/10.1016/j.jallcom.2018.03.114>.
- [17] N. Kumar, A. Shukla, N. Kumar, R.N.P. Choudhary, A. Kumar, Structural, electrical, and multiferroic characteristics of lead-free multiferroic: $Bi(Co_{0.5}Ti_{0.5})_3\cdot BiFeO_3$ solid solution, *RSC Adv.* 8 (2018) 36939–36950, <https://doi.org/10.1039/C8RA02306A>.
- [18] Z.L. Li, L.M. Jin, Z.Q. Cao, C. Zhang, X. Cao, G.R. Han, S. Peng, Y. Liu, Development and characterization of a novel RE^{3+} -doped Core-shell CeO_2 abrasive system and its glass CMP investigations, *Appl. Surf. Sci.* 638 (2023) 158055, <https://doi.org/10.1016/j.apsusc.2023.158055>.
- [19] L. Thansanga, A. Shukla, N. Kumar, R.N.P. Choudhury, Studies of structural, electrical and ferroelectric characteristics of gadolinium and yttrium modified bismuth ferrite, *Mater. Chem. Phys.* 263 (2021) 124359, <https://doi.org/10.1016/j.matchemphys.2021.124359>.
- [20] N. Kumar, A. Shukla, N. Kumar, R. Agarwal, R.N.P. Choudhury, Eco-friendly $Bi(Ni_{2/5}Ti_{2/5}Fe_{1/5})_3O_3$ nanoceramics: synthesis, dielectric and impedance studies, *Ceram. Int.* 47 (2021) 22147–22154, <https://doi.org/10.1016/j.ceramint.2021.04.237>.
- [21] N.Y. Kim, G. Kim, H. Sun, U. Hwang, J. Kim, D. Kwak, I.K. Park, T. Kim, J. Suhr, J. D. Nam, A nanoclustered ceria abrasives with low crystallinity and high Ce^{3+}/Ce^{4+} ratio for scratch reduction and high oxide removal rates in the chemical mechanical planarization, *J. Mater. Sci.* 57 (2022) 12318–12328, <https://doi.org/10.1007/s10853-022-07338-x>.
- [22] J. Liu, Z.Y. Zhang, C.J. Shi, Z. Ren, J.Y. Feng, H.X. Zhou, Z.S. Liu, F.N. Meng, S. M. Zhao, Novel green chemical mechanical polishing of fused silica through designing synergistic $CeO_2/h-BN$ abrasives with lubricity, *Appl. Surf. Sci.* 637 (2023) 157978, <https://doi.org/10.1016/j.apsusc.2023.157978>.
- [23] V.P. Singh, S.K. Patel, N. Kumar, B. Kurachen, Parametric effect on dissimilar friction stir welded steel-magnesium alloys joints: a review, *Sci. Technol. Weld. Join.* 24 (2019) 653–684, <https://doi.org/10.1080/13621718.2019.1567031>.
- [24] H.P. Xiao, S.H. Liu, 2D nanomaterials as lubricant additive: a review, *Mater. Des.* 135 (2017) 319–332, <https://doi.org/10.1016/j.matdes.2017.09.029>.
- [25] E. Koren, E. Lötscher, C. Rawlings, A.W. Knoll, U. Duerig, Adhesion and friction in mesoscopic graphite contacts, *Science* 348 (2015) 679–683, <https://doi.org/10.1126/science.aaa4157>.
- [26] J.C. Spear, B.W. Ewers, J.D. Batteas, 2D-nanomaterials for controlling friction and wear at interfaces, *Nano Today* 10 (2015) 301–314, <https://doi.org/10.1016/j.nantod.2015.04.003>.
- [27] Amaratunga Chhowalla, Thin films of fullerene-like MoS_2 nanoparticles with ultra-low friction and wear, *Nature* 407 (2000) 164–167, <https://doi.org/10.1038/35025020>.
- [28] O. Acikgoz, M.Z. Baykara, Speed dependence of friction on single-layer and bulk MoS_2 measured by atomic force microscopy, *Appl. Phys. Lett.* 116 (2020) 071603, <https://doi.org/10.1063/1.5142712>.
- [29] Y.Q. Guo, K. Xu, C.Z. Wu, J.Y. Zhao, Y. Xie, Surface chemical-modification for engineering the intrinsic physical properties of inorganic two-dimensional nanomaterials, *Chem. Soc. Rev.* 44 (2015) 637–646, <https://doi.org/10.1039/c4cs00302k>.
- [30] M. Chhowalla, H.S. Shin, G. Eda, L.J. Li, K.P. Loh, H. Zhang, The chemistry of two-dimensional layered transition metal dichalcogenide nanosheets, *Nat. Chem.* 5 (2013) 263–275, <https://doi.org/10.1038/nchem.1589>.
- [31] I. Lahouij, B. Vacher, J.M. Martin, F. Dassenoy, IF- MoS_2 based lubricants: influence of size, shape and crystal structure, *Wear* 296 (2012) 558–567, <https://doi.org/10.1016/j.wear.2012.07.016>.
- [32] I. Lahouij, F. Dassenoy, B. Vacher, J.M. Martin, Real time TEM imaging of compression and shear of single fullerene-like MoS_2 nanoparticle, *Tribol. Lett.* 45 (2012) 131–141, <https://doi.org/10.1007/s11249-011-9873-8>.
- [33] H. Yan, Y.C. Zhang, X.H. Niu, J.C. Wang, C.H. Yang, F. Luo, M.H. Qu, Y.H. Shi, R. Wang, Study on the surface interaction mechanism, corrosion inhibition effect and the synergistic action of potassium oleate and fatty alcohol polyoxy ethylene ether on copper film chemical mechanical polishing for giant large scale integrated circuit, *Thin Solid Films* 774 (2023) 139843, <https://doi.org/10.1016/j.tsf.2023.139843>.
- [34] D. Wang, L. Liu, Z.Y. Zhang, Q.B. Peng, C.J. Shi, X.Q. Liu, X.Y. Liu, H.X. Zhou, W. Wen, Atomic-scale planarization surface of quartz glass induced by novel green chemical mechanical polishing using three ingredients, *Materials Today Sustainability* 25 (2024) 100669, <https://doi.org/10.1016/j.mtsust.2024.100669>.
- [35] X.L. Shi, G.P. Chen, L. Xu, C.X. Kang, G.H. Luo, H.M. Luo, Y. Zhou, M.S. Dargusch, G.S. Pan, Achieving ultralow surface roughness and high material removal rate in fused silica via a novel acid SiO_2 slurry and its chemical-mechanical polishing mechanism, *Appl. Surf. Sci.* 500 (2020) 144041, <https://doi.org/10.1016/j.apsusc.2019.144041>.
- [36] Y. Dong, H. Lei, W.Q. Liu, Effect of mixed-shaped silica sol abrasives on surface roughness and material removal rate of zirconia ceramic cover, *Ceram. Int.* 46 (2020) 23828–23833, <https://doi.org/10.1016/j.ceramint.2020.06.159>.
- [37] L. Zhu, X. Jin, Y.Y. Zhang, S.X. Du, L. Liu, T. Rajh, Z. Xu, W.L. Wang, X.D. Bai, J. G. Wen, L.F. Wang, Visualizing anisotropic oxygen diffusion in ceria under activated conditions, *Phys. Rev. Lett.* 124 (2020) 056002, <https://doi.org/10.1103/PhysRevLett.124.056002>.
- [38] T. Liang, J.R. Hou, J.X. Xi, Mechanisms of nanofluid based modification MoS_2 nanosheet for enhanced oil recovery in terms of interfacial tension, wettability alteration and emulsion stability, *J. Dispersion Sci. Technol.* 44 (2021) 26–37, <https://doi.org/10.1080/01932691.2021.1930034>.
- [39] Y.G. Wang, L.C. Zhang, A. Biddut, Chemical effect on the material removal rate in the CMP of silicon wafers, *Wear* 270 (2011) 312–316, <https://doi.org/10.1016/j.wear.2010.11.006>.
- [40] S.J. Bai, J. Li, Y.X. Bi, J.Q. Yuan, S.M. Wen, Z. Ding, Adsorption of sodium oleate at the microfine hematite/aqueous solution interface and its consequences for flotation, *Int. J. Min. Sci. Technol.* 33 (2023) 105–113, <https://doi.org/10.1016/j.ijmst.2022.09.012>.
- [41] H. Ikeda, Y. Akagami, Highly efficient polishing technology for glass substrates using trib-co-chemical polishing with electrically controlled slurry, *J. Manuf. Process.* 15 (2013) 102–107, <https://doi.org/10.1016/j.jmapro.2012.11.002>.
- [42] E. Paparazzo, Use and mis-use of x-ray photoemission spectroscopy Ce3d spectra of Ce_2O_3 and CeO_2 , *J. Phys. Condens. Matter* 30 (2018) 343003, <https://doi.org/10.1088/1361-648X/ad248>.
- [43] S. Sahir, N.P. Yerriboina, S.Y. Han, K.M. Han, T.G. Kim, N. Mahadev, J.G. Park, Investigation of the effect of different cleaning forces on Ce-O-Si bonding during oxide post-CMP cleaning, *Appl. Surf. Sci.* 545 (2021) 149035, <https://doi.org/10.1016/j.apsusc.2021.149035>.
- [44] Y. Zhou, H.M. Luo, G.H. Luo, G.P. Chen, C.X. Kang, G.S. Pan, Chemical mechanical polishing (CMP) of fused silica (FS) using ceria slurry recycling, *ECS Journal of Solid State Science and Technology* 9 (2020) 044002, <https://doi.org/10.1149/2162-8777/ab8391>.
- [45] M. Green, Z.Q. Liu, P. Xiang, Y. Liu, M.J. Zhou, X.Y. Tan, F.Q. Huang, L. Liu, X. B. Chen, Doped, Conductive SiO_2 Nanoparticles for Large Microwave Absorption, vol. 7, *Light-Science & Applications*, 2018, p. 87, <https://doi.org/10.1038/s41377-018-0088-8>.
- [46] D. Sprenger, H. Bach, W. Meisel, P. Gütlich, XPS study of leached glass surfaces, *J. Non-Cryst. Solids* 126 (1990) 111–129, [https://doi.org/10.1016/0022-3093\(90\)91029-Q](https://doi.org/10.1016/0022-3093(90)91029-Q).
- [47] R. Popuri, H. Amanapu, C.K. Ranaweera, N.K. Baradanahalli, S.V. Babu, Potassium oleate as a dissolution and corrosion inhibitor during chemical mechanical planarization of chemical vapor deposited Co films for interconnect applications, *ECS Journal of Solid State Science and Technology* 6 (2017) P845–P852, <https://doi.org/10.1149/2.0251712jss>.
- [48] M.T. Wang, G.H. Huang, G.F. Zhang, Y.F. Chen, D.Z. Liu, C.B. Li, Selective flotation separation of fluorite from calcite by application of flaxseed gum as depressant, *Miner. Eng.* 168 (2021) 106938, <https://doi.org/10.1016/j.mineeng.2021.106938>.
- [49] A. Elimbi, S. Njouonkou, J.N. Nsami, P.D.B. Belibi, J.K. Mbadlam, Adsorption test of methylene blue onto porous powdered ceramics obtained from mixtures of kaolin-bauxite and kaolin-oyster shell, *Int. J. Environ. Sci. Technol.* 16 (2019) 1337–1350, <https://doi.org/10.1007/s13762-018-1754-3>.
- [50] Y. Chen, Z.N. Li, N.M. Miao, Polymethylmethacrylate (PMMA)/ CeO_2 hybrid particles for enhanced chemical mechanical polishing performance, *Tribol. Int.* 82 (2015) 211–217, <https://doi.org/10.1016/j.triboint.2014.10.013>.
- [51] N. Ozawa, M. Ishikawa, M. Nakamura, M. Kubo, Polishing process simulation of SiO_2 by CeO_2 abrasive grain under wet environment, *Hyomen Kagaku* 33 (2012) 351–356, <https://doi.org/10.1380/jsssj.33.351>.